

Refereed Proceedings

Heat Exchanger Fouling and Cleaning:

Fundamentals and Applications

Engineering Conferences International

Year 2003

Heat Exchanger Fouling in Phosphoric
Acid Evaporators - Evaluation of Field
Data -

R. M. Behbahani*

H. Müller-Steinhagen[†]

M. Jamialahmadi[‡]

*University of Surrey

[†]University of Stuttgart

[‡]University of Petroleum Industry - Ahwaz

This paper is posted at ECI Digital Archives.

<http://dc.engconfintl.org/heatexchanger/9>

HEAT EXCHANGER FOULING IN PHOSPHORIC ACID EVAPORATORS -EVALUATION OF FIELD DATA -

R. M. Behbahani¹, H. Müller-Steinhagen², M. Jamialahmadi³

¹Department of Chemical & Process Engineering, University of Surrey, Guildford, England
e-mail: r.behbahani@surrey.ac.uk

²Institute for Thermodynamics and Thermal Engineering, University of Stuttgart, Germany
Institute for Technical Thermodynamics, German Aerospace Research Centre, Stuttgart, Germany
e-mail: hans.mueller-steinhagen@dlr.de

³Research Department, University of Petroleum Industry, Ahwaz, Iran
e-mail: m.jamialahmadi@put.ac.ir

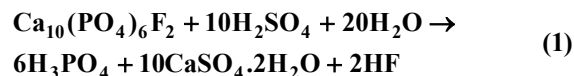
ABSTRACT

Multistage evaporators are frequently used in phosphoric acid plants to increase the concentration of dilute phosphoric acid to 52-55 wt% P₂O₅. The concentrated phosphoric acid solution is supersaturated with respect to calcium sulfate. As a result, part of the calcium sulfate in the liquor deposits on the heat exchanger tube walls. Since the thermal conductivity of these scales is very low, thin deposits can create a significant resistance to heat transfer. Therefore, regular cleaning of heat exchangers is required, frequently at less than biweekly intervals. As the major costs in modern phosphoric acid plants are the cost of energy, a thorough understanding of the fouling kinetics and of the effects of various operational parameters on the behavior of calcium sulfate is required to improve operation and design of the shell and tube heat exchangers, which are extensively used. In this investigation, a large number of heat exchanger data were collected from shell and tube heat exchangers of the phosphoric acid plant of the Razi Petrochemical Complex (Iran) and the fouling deposits were analyzed with respect to appearance and composition. The overall heat transfer coefficients and fouling resistances were evaluated at different times and a kinetic model for the crystallization fouling was developed. It is shown that the crystallization rate constant obeys an Arrhenius relationship with activation energy of 57 kJ/mol. The predictions of the suggested model are in good agreement with the plant data.

INTRODUCTION

Phosphoric acid is used mainly in the fertilizer field and other areas of chemical technology. In fertilizer production it serves as an intermediate between phosphate ore and major end products such as ammonium phosphate, triple super-phosphate, liquid mixed fertilizer, high-analysis solid mixed

fertilizer, and some types of nitric phosphate. Phosphoric acid is produced by two main processes: the wet process involving reaction of phosphate rock with sulfuric acid and the furnace process in which phosphorus is first produced, by reduction of phosphate rock, followed by oxidation and hydration to give phosphoric acid. Wet-process phosphoric acid, which contains the impurities found in the phosphate rock, is much important in fertilizer technology. Phosphoric acid for industrial and other uses that require high purity is usually produced by the furnace process. The major uses for furnace phosphoric acid are the manufacture of sodium phosphates and tetra-potassium pyrophosphate for use in detergents and calcium phosphates for use as an animal feed supplement and in drugs, glass, food, and plaster stabilizers. The main use for wet-process acid is in fertilizer production, where the impurities are not detrimental to any significant degree and sometimes even helpful. In this process phosphate rock is grounded to a particle size usually finer than 75µm and then digested in sulfuric acid at a temperature between 70 and 80 °C to yield phosphoric acid with a concentration of 27-30 wt % P₂O₅ and calcium sulfate dihydrate as by-product. The overall reaction is usually written as follows:



After the reaction section, phosphoric acid is separated from the calcium sulfate crystals by filtration. Multistage evaporators are then used to increase the concentration of the dilute phosphoric acid to 52-55 wt% P₂O₅. One of the evaporator heat exchangers is shown in Fig. 1. Because of scaling and corrosion, wet-process acid concentration presents many problems, which have not been entirely solved, despite major efforts in the past decades. The importance of this problem is indicated in Fig. 2.



Fig. 1 Graphite shell and tube heat exchanger



Fig. 2 Deposits on the heat exchanger head

The problems of scaling are essentially economic. Scaling of the heat exchanger surfaces has been of most concern because of reduced heat transfer rates and breakage of the fragile impregnated graphite tubes. As scaling becomes more serious, maintenance costs and downtime increase, while the production rate decreases. After some time of operation, the internal surfaces of equipment in contact with acid are covered with scale, which is removed by washing out with hot dilute sulfuric acid at high velocity. This descaling action is partly by dissolution and partly by abrasion. The main equipments which require regular washing are: flash chamber, heat exchangers, and acid pipework.

History of Phosphoric Acid Concentration

Previously, dilute phosphoric acid was being heated by steam coils in hooded pans with all equipment being made of lead to minimize corrosion (Slack, 1968). Rapid build-up of scale limited operation to a few hours, thus several units were necessary to maintain continuity of production while some of the coils and pans were being descaled by hot water. To avoid such problems, countercurrent heating by hot gas in spray towers was tried in the United States and Europe, but corrosion and air pollution, as well as P_2O_5 losses, limited the adoption of this method. Direct heating by a submerged flame or by a hot gas sparger was also used, but again, fume problems and P_2O_5 losses were major

handicaps. Batch-type vacuum concentrators were also developed for this purpose, although scaling limited continuous operation to short periods. Lead and lead-lined steel were the principal corrosion resistant materials used. Eventually, continuous vacuum evaporators were built that had external heat exchangers and employed internal, natural circulation. Rubber-lined, steel evaporator bodies and graphite heat exchanger tubes became virtually standard. Operating periods between descaling were increased to several days in many cases by including a small thickener in the evaporator system to remove precipitated impurities before they were deposited on the heat exchanger in the form of scale (Lutz, 1964). The use of Nionel alloy heater tubes in place of more fragile graphite ones subsequently became widespread, but unexplained failures led many producers to revert to graphite tubes. More recently, forced-circulation vacuum evaporators have become popular; the greater internal velocity provides better heat transfer.

Solubility of Calcium Sulfate in Phosphoric Acid Solutions

Solubility of calcium sulfate is very important with regards to the scaling problems during concentration. Calcium sulfate is encountered in three modifications: calcium sulfate anhydrite ($CaSO_4$), hemihydrate ($CaSO_4 \cdot 1/2 H_2O$) and dihydrate ($CaSO_4 \cdot 2H_2O$). The effects of the liquid composition and temperature on the stability of the different calcium sulfate modifications can be explained from the chemical potentials of AH (Anhydrite), HH (Hemihydrate), DH (Dihydrate) in the solid phase and in solution (Martynowics et al., 1996). The chemical potentials of AH, HH and DH in solution are defined as:

$$\mu_{AH(l)} = \mu^\circ + RT[\ln(\hat{a}_{Ca^{2+}} \cdot \hat{a}_{SO_4^{2-}})] \quad (2)$$

$$\mu_{HH(l)} = \mu^\circ + RT[\ln(\hat{a}_{Ca^{2+}} \cdot \hat{a}_{SO_4^{2-}} \cdot \hat{a}_{H_2O}^{1/2})] \quad (3)$$

$$\mu_{DH(l)} = \mu^\circ + RT[\ln(\hat{a}_{Ca^{2+}} \cdot \hat{a}_{SO_4^{2-}} \cdot \hat{a}_{H_2O}^2)] \quad (4)$$

where $\hat{a}_{Ca^{2+}}$, $\hat{a}_{SO_4^{2-}}$ and \hat{a}_{H_2O} represent the activities of the different ions in solution and μ° is defined as the chemical potential at standard conditions of 25 °C and 1 bar. At the solubility concentration of AH, the chemical potential of the solid, $\mu_{AH(s)}$, can be calculated from the thermodynamic solubility product, K_{sp} , using the following equation:

$$\mu_{AH(s)} = \mu^\circ + RT \ln(K_{sp, AH}) \quad (5)$$

Similar equations for the other hydrates can be given. In concentrated phosphoric acid, the water activity deviates from 1 and consequently, at the phase transition point, $\mu_{HH(s)}$ no longer equals $\mu_{DH(s)}$ but, instead, this point can be determined from the following equations:

$$\mu_{\text{HH(s)}} = \mu_{\text{HH(l)}} \quad (6)$$

$$\mu_{\text{DH(s)}} = \mu_{\text{DH(l)}}$$

Combining Eqs. (3), (4), (5) and (6) leads to:

$$RT \ln(K_{\text{sp}_{\text{HH}}}) = RT[\ln(\hat{a}_{\text{Ca}^{2+}} \cdot \hat{a}_{\text{SO}_4^{2-}} \cdot \hat{a}_{\text{H}_2\text{O}}^{\frac{1}{2}})] \quad (7)$$

$$RT \ln(K_{\text{sp}_{\text{DH}}}) = RT[\ln(\hat{a}_{\text{Ca}^{2+}} \cdot \hat{a}_{\text{SO}_4^{2-}} \cdot \hat{a}_{\text{H}_2\text{O}}^2)]$$

This set of equations can be simplified to:

$$\frac{K_{\text{sp}_{\text{DH}}}}{K_{\text{sp}_{\text{HH}}}} = \hat{a}_{\text{H}_2\text{O}}^{\frac{3}{2}} \quad (\text{at phase transition temperature}) \quad (8)$$

Because the solubility products of HH and DH are only a function of temperature, Eq. (8) shows that the phase transition temperature is exclusively determined by the water activity. Therefore, phosphoric acid affects the phase transition temperatures of the calcium sulfates just by changing the water activity. The water activity decreases at increasing phosphoric acid concentration, because the absolute amount of water decreases and because the water is coordinated by the phosphoric acid. This explains why the phase transition temperatures of the different calcium sulfate modification are a function of the phosphoric acid concentration. The stability of a crystal phase is related to its solubility; that is, the more stable phase is the less soluble one. Here, the solubility is defined as (Martynowics et al., 1996):

$$\text{Solubility} = S = \sqrt{[\text{Ca}^{2+}] \cdot [\text{SO}_4^{2-}]} \quad (9)$$

For HH and DH the solubilities can be written as:

$$S_{\text{HH}} = \sqrt{[\text{Ca}^{2+}] \cdot [\text{SO}_4^{2-}]} = \sqrt{\frac{K_{\text{sp}_{\text{HH}}}}{\gamma_{\text{Ca}^{2+}} \cdot \gamma_{\text{SO}_4^{2-}} \cdot \hat{a}_{\text{H}_2\text{O}}^{\frac{1}{2}}}} \quad (10)$$

$$S_{\text{DH}} = \sqrt{[\text{Ca}^{2+}] \cdot [\text{SO}_4^{2-}]} = \sqrt{\frac{K_{\text{sp}_{\text{DH}}}}{\gamma_{\text{Ca}^{2+}} \cdot \gamma_{\text{SO}_4^{2-}} \cdot \hat{a}_{\text{H}_2\text{O}}^2}} \quad (11)$$

Here \hat{a} indicates the activities of the ions; γ the respective activity coefficients; and K_{sp} the thermodynamic solubility product of either HH or DH. Any complex formation of the ions is included in their respective γ values. Because phosphoric acid strongly influences the water activity as well as the γ values of the calcium and sulfate ions, the solubilities of the calcium sulfate phases are also a strong function of the phosphoric acid concentration.

While there are plentiful data on the solubility of calcium sulfate in water, data on the solubility of this compound in phosphoric acid solutions is limited. Data are given by Taperova and Shulgina (1945), Linke (1965), Kurteva and Brutskus (1961), Zdanovskii and Vlasov (1971), and White and Mukhopadhyay (1990). Figure 3 shows some data from various sources for the transition temperature. The solubility curves prepared from data by Taperova and Shulgina (1945) are shown in Figure 4. These curves show that at temperatures higher than the equilibrium temperature the dihydrate and hemihydrate curves diverge more sharply at 32% P_2O_5 than at the two higher concentrations, and that the least divergence is obtained at the highest concentration. This means that at low phosphoric acid concentrations the nucleation threshold value is reached with less increase in temperature above the equilibrium temperature than at higher concentrations.

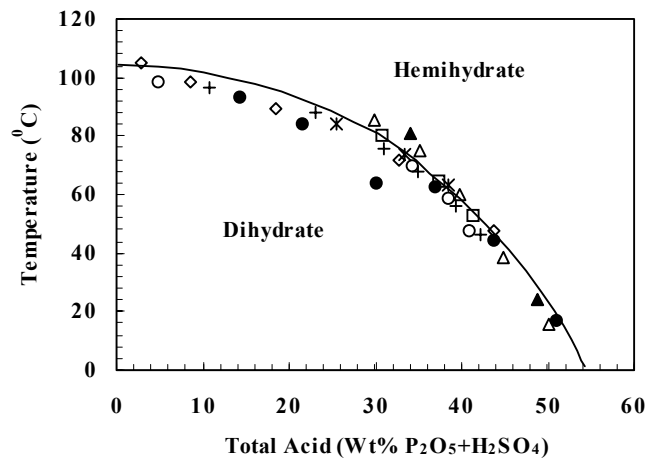


Fig. 3 Transition temp. versus total acid content

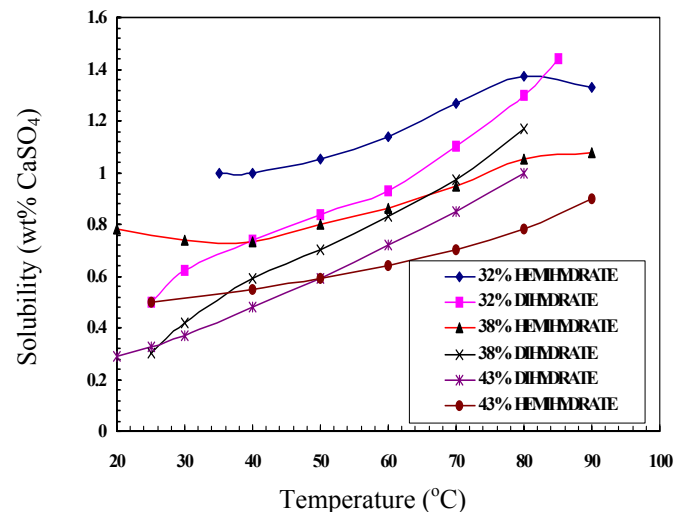


Fig. 4 Solubility of dihydrate and hemihydrate at various temperatures and P_2O_5 concentrations

PROCESS DESCRIPTION

Reaction

The flow diagram of the phosphoric acid plant is shown in Fig.5. The ground phosphate rock is fed to the compartment No. 1 where it is wetted and well dispersed by mixing with a portion of the return slurry from the flash cooler and most of the recycled acid from the filter. The phosphate rock is reacted in compartments No. 2 and No. 3. The major portion of the reaction is completed in compartment No. 4 and crystallization continues through compartments Nos. 5, 6, 7, 8 and 9 where the slurry is well degasified and in a condition of stability so that it may be easily pumped to the flash cooler. The attack tank temperature is controlled by recycling a large quantity of slurry cooled approximately by 4-5 °C in a flash cooler to

is determined each shift by the laboratory analysis of the discharge cake P_2O_5 and moisture content.

Evaporation

Product acid (29% P_2O_5) from the filter section is settled and stored. From storage it is fed continuously to three two-stage evaporators. The acid is concentrated from 29% to 42% in Stage I and then up to 53.5% in Stage II. Product acid (53.5% P_2O_5) is pumped from the Stage II units to clarification unit. The evaporator system has a total capacity to concentrate 1000 metric tons per day from 29% to 53.5%. Each evaporator unit (consisting of Stage I and Stage II evaporators) will concentrate one-third of the feed. Low pressure steam is used on the heaters, medium pressure steam on the ejectors and sea

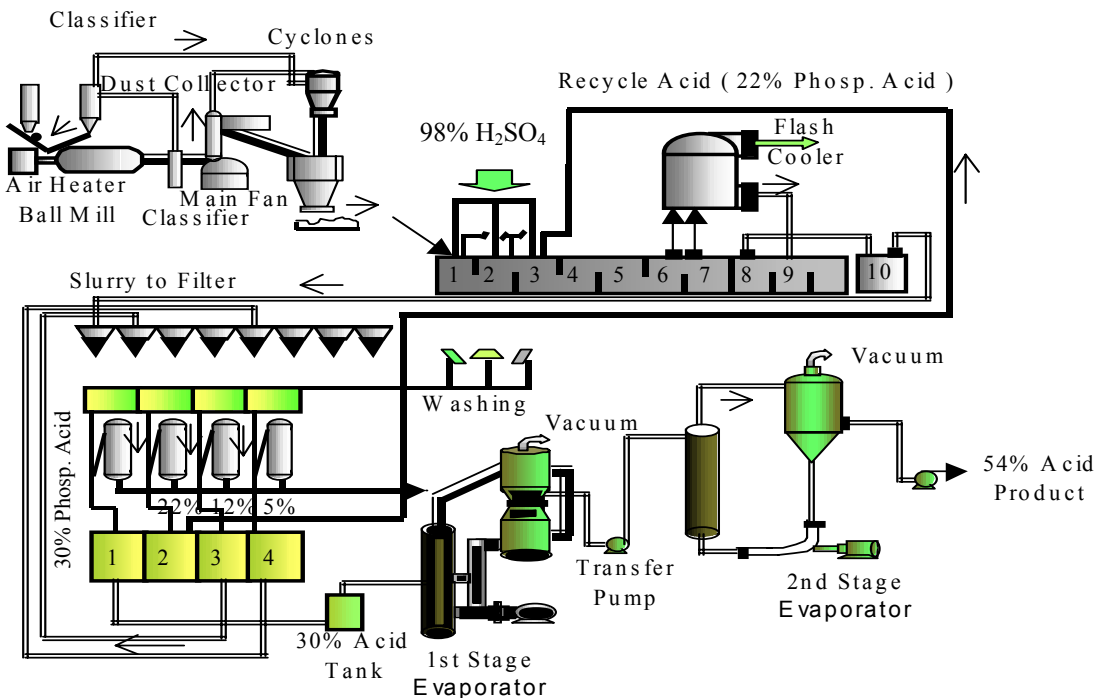


Fig. 5. The simplified flow diagram of wet-process phosphoric acid plant

the compartments No. 1 and No. 3. Feed acid for the flash cooler is obtained from the compartment No. 7.

Filtration

Slurry is pumped to the filter from the compartment No. 10. A flow control valve along with a stand-pipe arrangement in the return line to the attack tank assures that the feed rate is held constant. The feed rate is adjusted as required to keep a constant level in the attack tank. A constant slurry feed to the filter is essential for efficient operation and for maintaining good washing conditions and characteristics of the weak phosphoric acid recycle to the attack tank. Frequent checks for cake thickness, number of flooded pans, holes in cloth, and pan cleanliness are necessary for good operation. Wash water requirements are set by the washing efficiency of the three sequential filter washes. The effectiveness of the cake washing

water on the barometric condensers. Condensate from the heaters is saved and used for washing of the filter. Warm sea water overflows from hotwells (seal tanks) into trenches and is run by gravity to battery limits. When the heaters are new and the tubes are clean, it will be found that the pressure on the shell side of the heaters is very low, possibly down to 5 psig vacuum. As the units build up scale, the pressure will rise to a normal value of 5-8 psig. The operating pressure should never exceed 12 psig. When this pressure is reached, a boil-out will be necessary. The pressure safety valve is usually set at 20 psig.

EVALUATION OF FIELD DATA

The inlet and outlet temperatures (T_{in} and T_{out}) of the acid, the mass flow rate of the steam (M_{st}), the shell side

pressure (P_{shell}) and the shell side temperature (T_{shell}) were measured on the plant every 4 hours. The overall heat transfer coefficient in the plant, including both film resistances, is therefore calculated by a simple energy balance:

$$U = \frac{\dot{M}_{st} \Delta h_{st} (P_{shell})}{\Delta T_{lm} \cdot A} \quad (12)$$

with

$$\Delta T_{lm} = \frac{T_{out} - T_{in}}{\ln \frac{T_{st} - T_{in}}{T_{st} - T_{out}}} \quad (13)$$

Since no fouling will occur on the steam-side of the heat exchanger and the unit operates with constant heat duty, the fouling resistance on the liquor-side can be calculated from:

$$R_f = \frac{1}{U} - \frac{1}{U_0} \quad (14)$$

where U_0 is the overall heat transfer coefficient at the beginning and U is the heat transfer coefficient at some later time when fouling has taken place. Appropriate correlations for physical properties of crude phosphoric acid and steam were used from the comprehensive physical property data bank, which was prepared using the numerous data for phosphoric acid and steam which were collected from experimental measurements, valid references and industrial plant documents.

Results of Field Data Evaluation

During plant operation, the steam temperature (i.e. pressure) is not constant and increases continuously in order to maintain a constant heat flow rate. The surface temperature is calculated using the following simplified procedure:

- 1) The initial (clean) temperature at the interface between tube wall and process liquid is calculated including the heat transfer resistances on the condensation side and of the tube wall.
- 2) This temperature (inside of metal tube) is not constant with time, because the steam temperature increases. Even though flow velocity and surface roughness increase during scale formation, it still was assumed that the temperature at the interface between deposit and liquor (surface temperature) remains constant at the value of the clean heat transfer surface.

Typical heat transfer coefficients for different surface temperatures are plotted against time in Figure 6. The corresponding fouling resistances are plotted against time in Figure 7. The results show an almost linear increase with time. A linear relationship is generally characteristic of tough, hard, and adherent deposits. The deposit formation rate increases with increasing surface temperature.

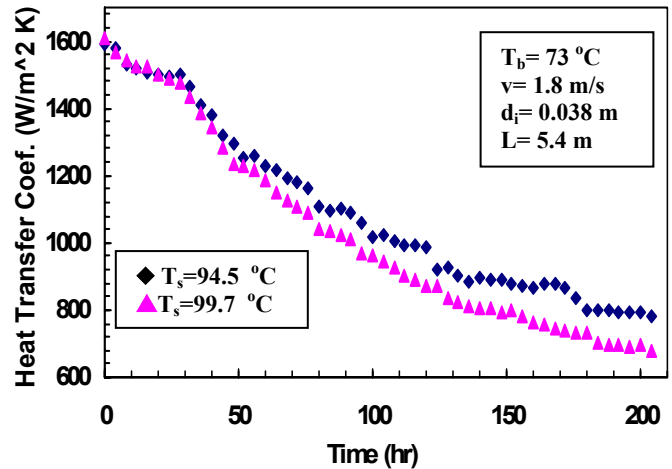


Fig. 6 Heat transfer coefficient as a function of time

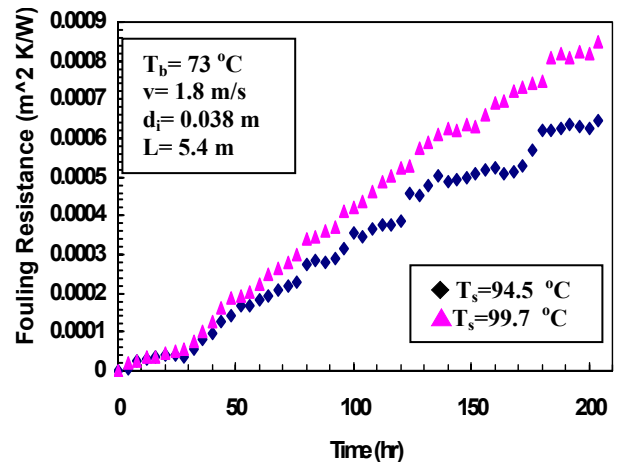


Fig. 7 Fouling resistance as a function of time

MODELING OF FOULING PROCESS

A segment of heat exchanger tube is shown in Figure 8. It can be analysed as a cylindrical one-dimensional system with negligible temperature gradients in axial direction. For steady state conditions with no internal heat generation, the appropriate cylindrical heat equation is:

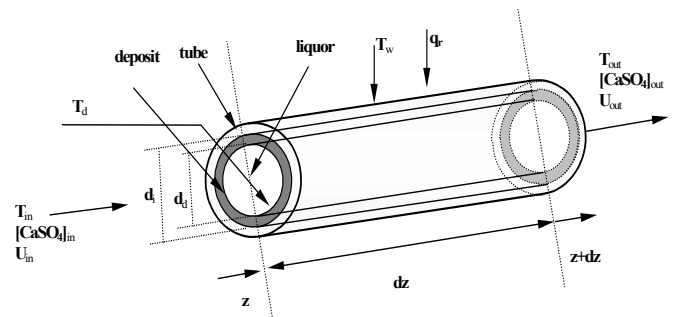


Fig. 8 A segment of heat exchanger tube

$$\frac{1}{r} \cdot \frac{d}{dr} (\lambda \cdot r \frac{dT}{dr}) = 0 \quad (15)$$

Considering Fourier's Law, the rate at which energy is conducted across the cylindrical surface is:

$$q_r = \lambda_d A_r \frac{dT}{dr} \quad (16)$$

or

$$q_r = 2\pi r L \lambda_d \frac{dT}{dr} \quad (17)$$

with the boundary conditions :

$$\begin{aligned} T &= T_i \quad \text{at } r = r_i \\ T &= T_d \quad \text{at } r = r_d \end{aligned} \quad (18)$$

The solution to Eq. (17) is :

$$q = \frac{2\pi \lambda_d L (T_i - T_d)}{\ln(r_i / r_d)} \quad (19)$$

$$\frac{q}{A_i} = \frac{\lambda_d (T_i - T_d)}{r_i \ln\left(\frac{r_i}{r_d}\right)}$$

Therefore, the thermal resistance for heat conduction through a cylindrical layer of deposit, which is identical to the scale resistance in this case, can be written as:

$$R_f = \frac{r_i \ln(r_i / r_d)}{\lambda_d} = \frac{d_i \ln\left(\frac{d_i}{d_d}\right)}{2\lambda_d} \quad (20)$$

The thickness of scale deposited for an incremental cross-sectional volume of the heated section can be predicted from the following equation:

$$\frac{d}{dt} (M_{CaSO_4, tot}) = \frac{d}{dt} (M_{CaSO_4, w}) + \frac{d}{dt} (M_{CaSO_4, b}) \quad (21)$$

$$= A_d K_w (C_{CaSO_4} - C^*_{CaSO_4})^2 + V K_b (C_{CaSO_4} - C^*_{CaSO_4})^2 \quad (22)$$

where M_{CaSO_4} is the mass of calcium sulfate precipitated, C_{CaSO_4} is the calcium sulfate concentration of the liquor, and $C^*_{CaSO_4}$ is the saturation calcium sulfate concentration. The saturation calcium sulfate solubility at different temperatures and phosphoric acid concentrations is calculated from the appropriate correlation derived using the solubility data. The reaction rate of the calcium sulfate crystallization is of second order with respect to the supersaturation (White and Mukhopadhyay, 1990). K_w is the

rate constant for surface deposition and is evaluated at T_w . All calcium sulfate precipitation described by this term is assumed to adhere onto the tube wall and hence to contribute to fouling on the heater surface. The second rate constant, K_b , is the volumetric rate constant for the bulk reaction, and is evaluated at T_b . All calcium sulfate precipitation predicted by the second term in Eq. (22) is assumed to nucleate in the bulk and remain in the liquor. The rate of change of scaled diameter with time is described by the following equation:

$$\frac{d}{dt} (d_d) = - \left(\frac{2}{A_d \cdot \rho_d \cdot fr_d} \right) \cdot \frac{d}{dt} (M_{CaSO_4, w}) = - \frac{2K_w}{\rho_d fr_d} (C_{CaSO_4} - C^*_{CaSO_4})^2 \quad (23)$$

fr_d is the average value for the mass fraction of the calcium sulfate in the deposit, which was obtained using the results of the analyses of the scale samples. Solving Eq. (23) with initial boundary conditions ($d_d(0) = d_i$) yields the scaled diameter as a function of time:

$$d_d(t) = d_i - \frac{2K_w}{\rho_d fr_d} (C_{CaSO_4} - C^*_{CaSO_4})^2 t \quad (24)$$

Substitution of Eq. (24) into Eq. (20) gives the time-dependent fouling resistance due to scale formation:

$$R_f(t) = d_i \cdot \frac{\ln \left[\frac{d_i}{d_i - 2 \frac{K_w}{\rho_d fr_d} (C_{CaSO_4} - C^*_{CaSO_4})^2 \cdot t} \right]}{2\lambda_d} \quad (25)$$

The surface reaction rate constant k_w is assumed to obey the Arrhenius equation:

$$k_w = k_0 \cdot \exp\left(\frac{-E_{act}}{RT_w}\right) \quad (26)$$

RESULTS OF THE FOULING MODELING

Fouling resistance data for all plant measurements were regressed to fit the model given in Eq. (25). Appropriate values of scale thermal conductivity, scale density, and calcium sulfate mass fraction were used ($\lambda_d = 0.73$ W/mK, $fr_d = 0.86$, $\rho_d = 2500$ kg/m³). The value of thermal conductivity has been confirmed from measurements using a thermal conductivity apparatus.

The results of the regression analyses of all measurements with different calcium sulfate concentration and T_w were plotted. The predicted K_w values collapsed to a

single function of T_w . This confirms the dependence of the reaction rate constant on the square of the calcium sulfate supersaturation. The natural logarithm of the rate constant was regressed as a function of $1/T_w$ and the Arrhenius temperature dependency was determined. The number of selected experiments was 4 and the temperature range covered 94.5 °C to 108 °C (13.5 °C apart). The activation energy evaluated for the surface reaction of the deposit formation is found to be 57 k J/mol.

The fouling resistance values calculated using the proposed model are compared with measured values in Fig. 9 for different surface temperatures. It is shown that the developed model predicts the measured fouling rates with reasonable accuracy.

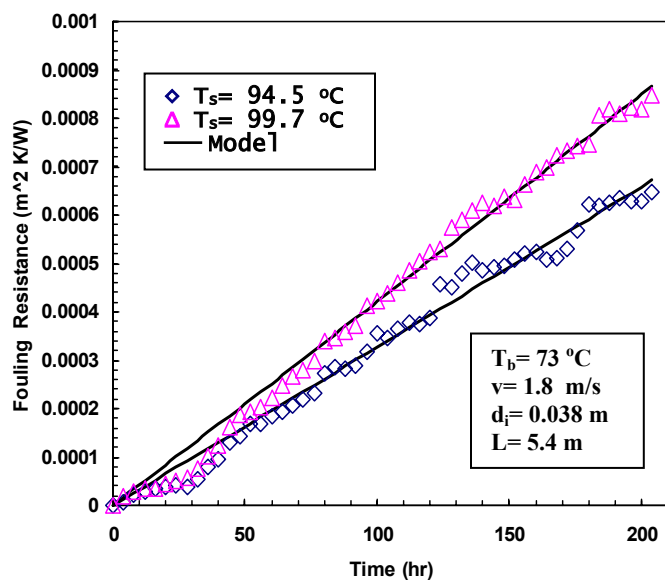


Fig. 9 Comparison of measured plant data with the proposed fouling model

DEPOSIT ANALYSIS

The elemental compositions of deposits were obtained with a S-3200n SEM energy-dispersive X-ray spectrometer system. Samples of the deposits were mounted in the desired orientation, i.e. upper or lower surface or cross-section, and placed under vacuum in the scanning electron microscope. The EDAX system is able to distinguish between different elements present in a sample by analyzing the energy of the X-rays given off. The technique is atomic weight sensitive. Therefore, errors are more pronounced for the low atomic weight elements. The EDAX system is able to detect all the elements down to sodium. Results for atomic weights below sodium are not reliable. A typical elemental analysis of the deposits is shown along with its respective scanning electron micrograph in Figure 10. The major elements identified are, calcium, sulphur and oxygen. The analysis shows that the deposits contain mainly calcium sulphate.

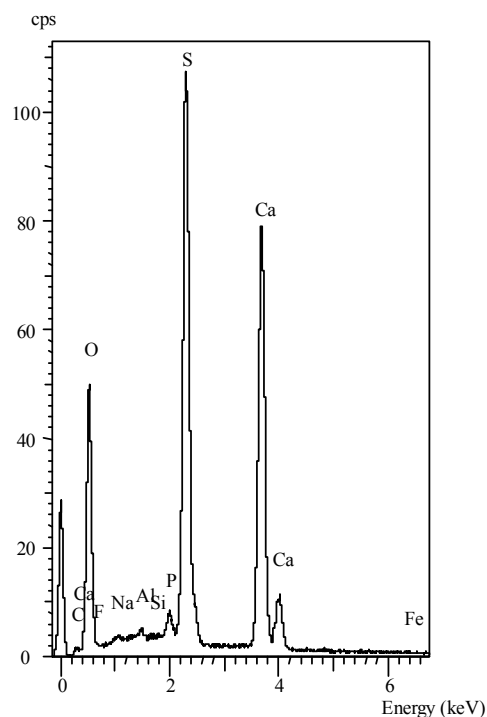


Fig. 10 Elemental analysis of deposits and corresponding scanning electron micrograph

CONCLUSIONS

Scaling is probably the main problem in phosphoric acid evaporators. While calcium sulfate has an inverted solubility in most neutral aqueous solutions, its solubility in phosphoric acid is of the normal type. Therefore, scaling on the heat transfer surfaces does not occur because of inverted solubility, but because of high supersaturation. A large number of plant operating data of the heat exchangers of the phosphoric acid evaporation unit at the Razi Petrochemical Complex (Iran) were collected every 4 hours for more than 50 runs, each run about 8-12 days. Heat transfer coefficients and fouling rates were evaluated. A linear increase of fouling resistance with time has been observed which is a result of crystallization fouling. The dependence of the reaction rate constant on the square of the calcium sulfate supersaturation has been confirmed. A kinetic model for the crystallization fouling was developed. It has been shown

that the crystallization rate constant obeys an Arrhenius relationship with an activation energy of 57 kJ/mol. The predictions of the suggested model are in good agreement with the plant operating data. The fouling deposits were analyzed and it was found that the deposits contain mainly calcium sulphate.

ACKNOWLEDGEMENTS

The support of the presented investigations by Razi Petrochemical Complex is gratefully acknowledged.

NOMENCLATURE

A	heat transfer area, m ²
\hat{a}	activity
C	concentration, kg/m ³
d	diameter, m
E _{act}	activation energy, J/mol
fr	mass fraction
h	latent heat, J/kg
K _b	bulk reaction rate constant, m ³ /kg s
K _{sp}	solubility product
K _w	surface scaling reaction rate constant, m ⁴ /kg s
L	length, m
M	mass flow rate, kg/s
m	mass, kg
P	pressure, Pa
q	heat transfer rate, W
R	universal gas constant, J/mol K
R _f	fouling resistance, m ² K/W
r	radial, m
T	temperature, °C or K
t	time, s
U	Overall heat transfer coefficient (based on inside area), W/m ² K
V	volume, m ³
v	velocity, m/s
δ	scale thickness, m
γ	activity coefficient
λ	thermal conductivity, W/m K
μ	chemical potential, J/mol
ρ	density, kg/m ³

Subscripts

AH	anhydrite
b	bulk
Ca ²⁺	calcium ion

CaSO ₄	calcium sulfate
d	deposit
DH	dihydrate
f	fouling
H ₂ O	water
HH	hemihydrate
i	inside
in	inlet
lm	log mean
out	outlet
r	radial
s	surface
SO ₄ ²⁻	sulfate ion
st	steam
t	at time t
tot	total
w	wall

Superscripts

*	saturation
---	------------

REFERENCES

- Kurteva, O.I. , Brutskus, E.B. ,1961, J. Appd Chem. USSR, 34(8), 1636.
- Linke, W.F., 1965, Solubilities of Inorganic and Metal Organic Compounds, Amer. Chem. Soc., Washington, 4th ed., vol. 1.
- Lutz W. A. (to Dorr-Oliver, Inc.), 1964 , U.S. Pat. 3,148,948.
- Martynowics, E.T.M.J., Witkamp, G.J., Van Rosmalen, G.M., 1996, "The Effect of Aluminum Fluoride on the Formation of Calcium Sulfate Hydrates", Hydrometallurgy, 41, pp. 171-186.
- Slack, V., 1968, Phosphoric Acid, Marcel Dekker, New York, pp.331-342.
- Taperova, A.A. , Shulgina, M.N., 1945, J. Appd. Chem. USSR, 18(9), 521.
- White, E. T. and Mukhopadhyay, S., 1990, "Crystallization of gypsum from phosphoric acid solutions", ACS Symposium Series 438, pp. 292-315.
- Zdanovskii, A.B., Vlasov, G.A., 1971, J. Appd. Chem. USSR , 44(1),15.